

Synthesis, Structures, and Physical Properties of Copper(II)–Gadolinium(III) Complexes Combining Ferromagnetic Coupling and Quadratic Nonlinear Optical Properties

Olivier Margeat, Pascal G. Lacroix,* Jean Pierre Costes, Bruno Donnadieu, and Christine Lepetit

Laboratoire de Chimie de Coordination du CNRS, 205 route de Narbonne, 31077 Toulouse, France

Keitaro Nakatani

PPSM-UMR 8531, Ecole Normale Supérieure de Cachan, Avenue du Président Wilson, 94235 Cachan, France

Received February 16, 2004

Two copper(II)–gadolinium(III) metal complexes of formula $\text{Cu}^{\text{II}}\text{Gd}^{\text{III}}\text{LX}_3$ are reported. H_2L stands for the Schiff base ligand obtained by condensation of 3,4-dimethoxysalicylaldehyde with ethylenediamine (complex **1**) or 1*R*,2*R*-(+)-1,2-diphenylethylenediamine (complex **2**). While **1** reveals a centrosymmetric crystal structure, **2** crystallizes in the noncentrosymmetric $P2_12_12_1$ space group and exhibits an efficiency 0.3 time that of urea in second harmonic generation. Due to a trend for dissociation in solution, the molecular hyperpolarizabilities (β) cannot be determined experimentally for **1** and **2**. Nevertheless, the electric field induced second harmonic (EFISH) technique, in connection with spectroscopic data and a ZINDO semiempirical approach, leads to a β value of $-6.5 \times 10^{-30} \text{ cm}^5 \text{ esu}^{-1}$, for the related $\text{Cu}^{\text{II}}\text{L}$ monomers, as an indicative range of magnitude in all these Schiff base complexes. In addition, **1** and **2** exhibit a ferromagnetic coupling in solid state with $J = 3.3$ and 1.3 cm^{-1} , respectively (J being the parameter of the exchange Hamiltonian $\hat{H} = -J\hat{S}_{\text{Cu}} \cdot \hat{S}_{\text{Gd}}$).

Introduction

The past decade has witnessed a growing interest for multiproperty molecular materials, in relation to the emerging concept of molecular switch.^{1,2} In the area of quadratic nonlinear optical (NLO) properties, several switchable chromophores have recently been reported.³ In most cases, the modulation of the property is monitored by a proton transfer,⁴ an isomerization,⁵ or a redox process,⁶ which implies a

chemical modification to some extent and, hence, a modification of all molecular parameters, among which is the quadratic hyperpolarizability (β). Another approach would be to introduce an additional (e.g. magnetic) property on a single molecular entity, connected to the optical property in some way. In that case the additional property could hopefully interact and eventually modulate the NLO response, the molecule being unaffected.

In molecular nonlinear optics, organic chromophores exhibiting “closed-shell” diamagnetic electronic structures have by far been the most widely investigated class of materials.⁷ By contrast, relatively few inorganic derivatives have been investigated,⁸ even if some of them have exhibited extremely large NLO responses.^{9,10} Nevertheless, several studies conducted in the past decade have suggested that

* Author to whom correspondence should be addressed. E-mail: pascal@lcc-toulouse.fr.

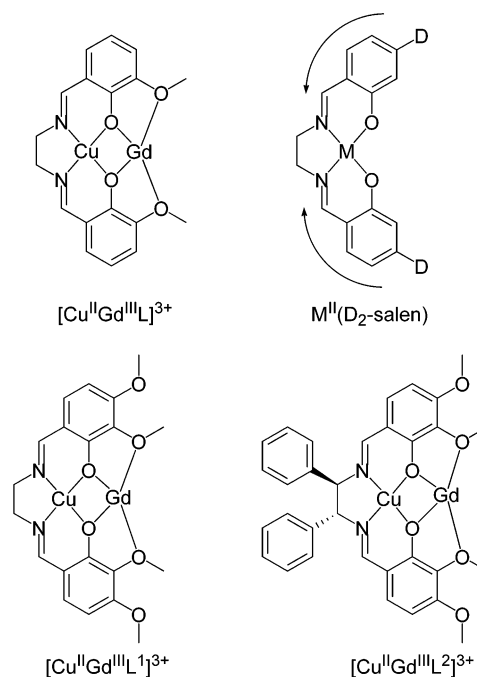
- (1) Lehn, J. M. *Supramolecular Chemistry-Concepts and Perspectives*; VCH: Weinheim, Germany, 1995.
- (2) Ward, M. D. *Chem. Soc. Rev.* **1995**, *24*, 121.
- (3) For a review on quadratic NLO switch, see: Coe, B. *Chem.—Eur. J.* **1999**, *5*, 2464.
- (4) (a) Houbrechts, S.; Clays, K.; Persoons, A.; Pikramenou, Z.; Lehn, J. M. *Chem. Phys. Lett.* **1996**, *258*, 485. (b) Nakatani, K.; Delaire, J. A. *Chem. Mater.* **1997**, *9*, 2682.
- (5) (a) Loucif-Saïbi, R.; Nakatani, K.; Delaire, J. A.; Dumont, M.; Sekkat, Z. *Chem. Mater.* **1993**, *5*, 229. (b) Gilat, S. L.; Kawai, S. H.; Lehn, J. M. *Chem.—Eur. J.* **1995**, *1*, 275.
- (6) Coe, B. J.; Houbrechts, S.; Asselberghs, I.; Persoons, A. *Angew. Chem., Int. Ed.* **1999**, *38*, 366.

- (7) *Nonlinear Optics of Organic Molecules and Polymers*; Nalwa, H. S., Miyata, S., Eds.; CRS Press: New York, 1997.
- (8) For reviews on inorganic complexes with NLO properties, see for example: (a) Di Bella, S. *Chem. Soc. Rev.* **2001**, *30*, 355. (b) Lacroix, P. G. *Eur. J. Inorg. Chem.* **2001**, 339.
- (9) Le Bozec, H.; Renouard, T. *Eur. J. Inorg. Chem.* **2000**, 229.

paramagnetic species should be intriguing NLO chromophores. For instance, Di Bella has shown that on passing from closed-shell Ni^{II} (salophen) to open-shell Cu^{II} and Co^{II} analogues, experimental β values could increase from -20×10^{-30} to -50×10^{-30} and $-170 \times 10^{-30} \text{ cm}^5 \text{ esu}^{-1}$.¹¹ Additional investigations have also implemented the idea that unpaired electrons could lead to enlarged NLO responses, for instance, in radicals.^{12,13} More recently, we have investigated the possibility for quadratic modulation obtained upon spin crossover ($S = 0 \rightarrow 2$) behavior in an iron(II) derivative and provided computational evidence for larger β value associated with the higher spin state.¹⁴ We have also reported on a sizable NLO modulation induced by Faraday rotation, occurring when a laser beam propagates in a magnetized material.¹⁵ All together, these investigations lead to the suggestion that there is a potential interest in trying to design molecular materials in which ferromagnetism and quadratic NLO response would take place.

As a first step toward this goal, we wish to report here on a family of copper(II)–gadolinium(III) metal complexes in which both ferromagnetic coupling and quadratic NLO properties are observed for the first time. Our group has developed a general route to binuclear $\text{Cu}^{\text{II}}\text{Gd}^{\text{III}}\text{LX}_3$ complexes, in which H_2L is the ligand obtained from the Schiff base condensation of 3-methoxysalicylaldehyde and 1,2-ethylenediamine (Chart 1).¹⁶ Interestingly, the magnetic properties reveal a general trend for ferromagnetic coupling between the $S = 1/2$ copper(II) and the $S = 7/2$ gadolinium(III) atoms, in these systems. However, despite a non-centrosymmetric molecular structure, these complexes do not exhibit the “push–pull” electronic structure required for observable quadratic NLO response. By contrast, several reports have pointed out that substituted metal(salen) complexes exhibit sizable NLO response when a donor (D) substituent is present in the para position, with respect to the withdrawing imine group (Chart 1).^{17,18} Following this idea, we have designed new ligands, containing several methoxy groups, to ensure both the anchorage of the copper–gadolinium magnetic core and the “push–pull” character required for an observable optical nonlinearity. These ligands, labeled H_2L^1 and H_2L^2 (Chart 1), possess the same π -electronic core and, therefore, are expected to lead to the same

Chart 1



molecular properties. On the other hand, H_2L^2 is a chiral molecule built from a pure (1*R*,2*R*) enantiomer, which has been selected to force the crystallization of the related $\text{Cu}^{\text{II}}\text{Gd}^{\text{III}}$ complex in a noncentrosymmetric space group, to favor the observation of a bulk NLO response in solid state.

The synthesis and crystal structures of the $\text{Cu}^{\text{II}}\text{Gd}^{\text{III}}$ binuclear species will be presented first. Then their experimental NLO responses and magnetic properties will be presented successively.

Experimental Section

Starting Materials and Equipment. 3,4-Dimethoxysalicylaldehyde was synthesized according to the procedure previously described.¹⁹ Any other starting materials were purchased from Aldrich, except (1*R*,2*R*)-(+)-1,2-diphenylethylenediamine (Fluka), and were used as received. UV–visible spectra were recorded on a Hewlett-Packard 8452 A spectrophotometer. Elemental analyses were performed by the Service de Microanalyses du CNRS, Laboratoire de Chimie de Coordination, Toulouse, France. Thermal measurements were performed by TGDTA92 thermoanalyzer. Magnetic susceptibility data were collected using a SQUID-based magnetometer on a QUANTUM Design model MPMS instrument. All data were corrected for diamagnetism estimated from Pascal’s constants.²⁰

Synthesis. 3,4-Dimethoxysalicylaldehyde. In a well-stirred solution of 5.28 g (2.7×10^{-2} mol) of 2,3,4-trimethoxybenzaldehyde in 40 mL of dry toluene was slowly added 3.59 g (2.7×10^{-2} mol) of AlCl_3 . The resulting red mixture was heated at 80 °C for 4 h and then allowed to cool to room temperature. After addition of 40 mL of a cold solution of HCl (5 M), the aqueous phase was extracted with 3×25 mL of CHCl_3 , washed with 25 mL of HCl (3 M), and then extracted with 2×25 mL of NaOH (10%). Slow addition of concentrated HCl in the aqueous phase allowed 3.04 g

- (10) (a) LeCours, S. M.; Guan, H. W.; Di Magno, S. G.; Wang, C. H.; Therien, M. J. *J. Am. Chem. Soc.* **1996**, *118*, 1497. (b) Priyadarshy, S.; Therien, M. J.; Beratan, D. N. *J. Am. Chem. Soc.* **1996**, *118*, 1504.
- (11) Di Bella, S.; Fragalà, I.; Ledoux, I.; Marcks, T. J. *J. Am. Chem. Soc.* **1995**, *117*, 9481.
- (12) Di Bella, S.; Fragalà, I.; Marks, T. J.; Ratner, M. A. *J. Am. Chem. Soc.* **1996**, *118*, 8, 12747.
- (13) Malfant, I.; Cordente, N.; Lacroix, P. G.; Lepetit, C. *Chem. Mater.* **1998**, *10*, 4079.
- (14) Averseng, F.; Lacroix, P. G.; Lepetit, C.; Tuchagues, J. P. *Chem. Mater.* **2000**, *12*, 2225.
- (15) Lacroix, P. G.; Malfant, I.; Bénard, S.; Yu, P.; Rivière, E.; Nakatani, K. *Chem. Mater.* **2001**, *13*, 441.
- (16) Costes, J. P.; Dahan, F.; Dupuis, A.; Laurent, J. P. *Inorg. Chem.* **1997**, *36*, 3429.
- (17) (a) Di Bella, S.; Fragalà, I.; Ledoux, I.; Zyss, J. *Chem.—Eur. J.* **2001**, *7*, 3738. (b) Di Bella, S.; Fragalà, I.; Ledoux, I.; Diaz Garcia, M. A.; Marks, T. J. *J. Am. Chem. Soc.* **1997**, *119*, 9550.
- (18) (a) Averseng, F.; Lacroix, P. G.; Malfant, I.; Dahan, F.; Nakatani, K. *J. Mater. Chem.* **2000**, *10*, 1013. (b) Lacroix, P. G.; Di Bella, S.; Ledoux, I. *Chem. Mater.* **1996**, *8*, 541.

(19) Chantimakorn, V.; Nimgirawath, S. *Aust. J. Chem.* **1989**, *42*, 209.

(20) Earnshaw, A. *Introduction to Magnetochemistry*; Academic Press: London, 1968.

of 3,4-dimethoxysalicylaldehyde as a slight yellow precipitate (62% yield). $^1\text{H NMR}$ (CDCl_3): δ 3.871 (s, 3H), 3.921 (s, 3H), 6.579 (d, 8.8 Hz, 1H), 7.266 (d, 8.8 Hz, 1H), 9.714 (s, 1H), 11.18 (s, 1H).

$\text{CuL}^1 \cdot \text{H}_2\text{O}$. To a solution of 83 mg (1.38×10^{-3} mol) of ethylenediamine and 503 mg (2.76×10^{-3} mol) of 3,4-dimethoxysalicylaldehyde in 50 mL of absolute ethanol were successfully added 235 mg (1.38×10^{-3} mol) of $\text{CuCl}_2 \cdot 2\text{H}_2\text{O}$ and 280 mg (2.76×10^{-3} mol) of Et_3N . The mixture was heated under reflux for 4 days and then concentrated under vacuum. After cooling to -10°C , the resulting precipitate was filtered off, washed with ethanol, and dried under vacuum (yield 75%). Anal. Calcd for $\text{C}_{20}\text{H}_{22}\text{CuN}_2\text{O}_6 \cdot \text{H}_2\text{O}$: C, 51.33; H, 5.60; N, 5.99. Found: C, 51.08; H, 4.66; N, 6.17.

NiL^1 . The procedure is the same as that of the previous $\text{CuL}^1 \cdot \text{H}_2\text{O}$ complex, except that $\text{NiCl}_2 \cdot 6\text{H}_2\text{O}$ was used instead of $\text{CuCl}_2 \cdot 2\text{H}_2\text{O}$, as the starting metal salt (yield 69%). Anal. Calcd for $\text{C}_{20}\text{H}_{22}\text{NiO}_6$: C, 53.96; H, 4.98; N, 6.30. Found: C, 53.81; H, 4.37; N, 6.14.

$\text{CuGdL}^1(\text{NO}_3)_{2.5}(\text{OH})_{0.5}(\text{H}_2\text{O}) \cdot 0.5\text{H}_2\text{O}$ (1). To a black suspension of 90 mg (1.92×10^{-4} mol) of $\text{CuL}^1 \cdot \text{H}_2\text{O}$ in 10 mL acetone was added 113 mg (2.5×10^{-4} mol) of $\text{Gd}(\text{NO}_3)_3 \cdot 6\text{H}_2\text{O}$. The resulting mixture was refluxed for 1 day and then allowed to cool to room temperature. The resulting brown solid was filtered off, washed with acetone and ether, and dried under vacuum (yield 25%). Anal. Calcd for $\text{C}_{20}\text{H}_{25.5}\text{CuGdN}_{4.5}\text{O}_{15.5}$: C, 30.11; H, 3.22; N, 7.90. Found: C, 30.17; H, 3.16; N, 7.38. Single crystals were obtained by slow evaporation in acetone.

$\text{CuL}^2 \cdot 0.5\text{H}_2\text{O}$. To a solution of 106 mg (5×10^{-4} mol) of 1*R*,2*R*-(+)-1,2-diphenylethylenediamine in 20 mL of absolute ethanol were added 85.3 mg (5×10^{-4} mol) of $\text{CuCl}_2 \cdot 2\text{H}_2\text{O}$, 182 mg (10^{-3} mol) of 3,4-dimethoxysalicylaldehyde, and 101 mg (10^{-3} mol) of Et_3N . The mixture was heated under reflux for 4 days and then concentrated and cooled to -10°C . The resulting precipitate was filtered off, washed with ethanol, and dried under vacuum (yield 52%). Anal. Calcd for $\text{C}_{32}\text{H}_{30}\text{CuN}_2\text{O}_6 \cdot 0.5\text{H}_2\text{O}$: C, 62.88; H, 5.11; N, 4.58. Found: C, 62.45; H, 4.81; N, 4.32.

$\text{CuGdL}^2(\text{NO}_3)_3$ (2). To a greenish suspension of 110 mg (1.8×10^{-4} mol) of $\text{CuL}^2 \cdot 1/2\text{H}_2\text{O}$ in 10 mL of acetone was added 113 mg (2.5×10^{-4} mol) of $\text{Gd}(\text{NO}_3)_3 \cdot 6\text{H}_2\text{O}$. The mixture was heated under reflux for 1 day and then the resulting solution was concentrated and cooled to -10°C . The resulting precipitate was filtered off, washed with acetone and ether, and then dried under vacuum (yield 30%). Anal. Calcd for $\text{C}_{32}\text{H}_{30}\text{CuGdN}_5\text{O}_{15}$: C, 40.65; H, 3.20; N, 7.41. Found: C, 40.12; H, 3.32; N, 6.71. Single crystals were obtained by slow evaporation in acetone.

X-ray Crystal Structure Determination. Data were collected at low-temperature $T = 180\text{ K}$ on a Stoe imaging plate diffraction system (IPDS) equipped with an Oxford Cryosystems cooler device. Final unit cell parameters were obtained by the least-squares refinement of 8000 reflections.

The structures were solved by direct methods using (SIR92)²¹ and refined by least-squares procedures on F^2 using SHELXL-97²² included in WinGX programs.²³ All hydrogens atoms were located on a difference Fourier map, but they were introduced in calculation

Table 1. Crystallographic Data for $\text{CuGdL}^1(\text{NO}_3)_{2.5}(\text{OH})_{0.5}(\text{H}_2\text{O}) \cdot 0.5\text{H}_2\text{O}$ (1) and $\text{CuGdL}^2(\text{NO}_3)_3 \cdot \text{C}_3\text{H}_6\text{O}$ (2)

| | 1 | 2 |
|------------------------------------|---|---|
| empirical formula | $\text{C}_{20}\text{H}_{25}\text{CuGdN}_{4.5}\text{O}_{15.5}$ | $\text{C}_{35}\text{H}_{36}\text{CuGdN}_5\text{O}_{16}$ |
| fw | 796.7 | 1003.48 |
| cryst system | triclinic | orthorhombic |
| space group | $P\bar{1}$ | $P2_12_12_1$ |
| <i>a</i> , Å | 11.026(2) | 10.7725(9) |
| <i>b</i> , Å | 11.174(2) | 18.2789(17) |
| <i>c</i> , Å | 12.271(2) | 22.9876(19) |
| α , deg | 105.07(2) | 90 |
| β , deg | 103.13(2) | 90 |
| γ , deg | 101.50(2) | 90 |
| <i>V</i> , Å ³ | 1366.4(10) | 4526.5(7) |
| <i>Z</i> | 2 | 4 |
| <i>T</i> , K | 180(2) | 180(2) |
| λ , Å | 0.710 73 | 0.710 73 |
| ρ (calcd), g cm ⁻³ | 1.935 | 1.473 |
| no. of reflns colld | 9276 | 23638 |
| no. of reflns used | 3707 [$R(\text{int}) = 0.0422$] | 5699 [$R(\text{int}) = 0.1198$] |
| no. of params | 410 | 568 |
| R ($I > 2\sigma(I)$) | 0.0264 | 0.0557 |
| R_w ($I > 2\sigma(I)$) | 0.0657 | 0.1177 |

in idealized positions with an isotropic thermal parameter fixed at 20% higher than those of the carbons atoms to which they were connected. All non-hydrogen atoms were anisotropically refined. For the compound $\text{CuGdL}^1(\text{NO}_3)_{2.5}(\text{OH})_{0.5}(\text{H}_2\text{O}) \cdot 0.5\text{H}_2\text{O}$, some statistical disorders were observed, between NO_3^- and OH^- groups which connect two $\text{Cu}^{\text{II}}\text{Gd}^{\text{III}}$ units and were found disordered on both sides of an inversion center and for a NO_3^- group for which one oxygen atom was found statistically disordered on two positions with a ratio of occupancy equal to 0.5.

The drawing of the molecules were realized with the help of ORTEP32,²⁴ and the atomic scattering factors were taken from ref 25. Further details on the crystal structure investigation are available on request from the Director of the Cambridge Crystallographic Data Center, 12 Union Road, GB-Cambridge, CB21EZ U.K., on quoting the full journal citation. Details of data collection and refinement are given in Table 1.

Theoretical Methods. The all-valence INDO (intermediate neglect of differential overlap) method²⁶ was employed for the calculation of the electronic spectra for the mononuclear species. The monoexcited configuration interaction (MECI) approximation was employed to describe the excited states. The 100 lowest energy one-electron transitions between the 10 highest occupied molecular orbitals and the 10 lowest unoccupied ones were chosen to undergo CI mixing. Calculations were performed using the INDO/1 Hamiltonian incorporated in the commercially available MSI software package ZINDO.²⁷ The geometry of CuL^1 and NiL^1 was calculated using molecular mechanics (MM) and the extensible systematic force field (ESFF) of Discover.²⁸ This force field is able to reproduce quite accurately the X-ray crystal structure of related Ni^{II} and Cu^{II} complexes,^{18,29} with an averaged uncertainty of 0.03 Å (bond lengths) and 1.5 deg (angles). The MM-calculated geometry of CuL^1 and NiL^1 appears therefore reliable enough to

(21) Altomare, A.; Cascarano, G.; Giacovazzo, G.; Guagliardi, A.; Burla, M. C.; Polidori, G.; Camalli, M. SIR92-a program for automatic solution of crystal structures by direct methods. *J. Appl. Crystallogr.* **1994**, *27*, 435.

(22) Sheldrick, G. M. SHELX97 [Includes SHELXS97, SHELXL97, CIFTAB]-Programs for Crystal Structure Analysis (Release 97-2); Institut für Anorganische Chemie der Universität: Tammanstrasse 4, D-3400 Göttingen, Germany, 1998.

(23) WINGX; Farrugia, L. J. *J. Appl. Crystallogr.* **1999**, *32*, 837.

(24) ORTEP3 for Windows; Farrugia, L. J. *J. Appl. Crystallogr.* **1997**, *30*, 565.

(25) *International Tables for X-ray Crystallography*; Kynoch Press: Birmingham, England, 1974; Vol. IV.

(26) (a) Zerner, M. C.; Loew, G.; Kirchner, R.; Mueller-Westerhoff, U. J. *Am. Chem. Soc.* **1980**, *102*, 589. (b) Anderson, W. P.; Edwards D.; Zerner, M. C. *Inorg. Chem.* **1986**, *25*, 2728.

(27) ZINDO, release 96.0; Molecular Simulations Inc.: Cambridge, U.K., 1996.

(28) Discover, release 95.0; Biosym Technologies: San Diego, CA, 1996.

(29) Yao, H. H.; Huang, W. T.; Lo, J. M.; Liao, F. L.; Wang, S. L. *Eur. J. Solid State Inorg. Chem.* **1997**, *34*, 3355.

estimate the electronic spectra, and the corresponding hyperpolarizabilities using ZINDO. The spectroscopic features being grossly identical for both derivatives, the origin of the NLO response was therefore assumed to be the same in term of electronic transition for both complexes.

The magnetic susceptibility has been computed by exact calculation of the energy levels associated to the spin Hamiltonian through diagonalization of the full matrix with a general program for axial symmetry.³⁰ Least-squares fittings were accomplished with an adapted version of the function-minimization program MINIUT.³¹

NLO Properties. The principle of the electric field induced second harmonic (EFISH) technique is reported elsewhere.^{32,33} The data were recorded using a picosecond Nd:YAG pulsed (10 Hz) laser operating at $\lambda = 1.064 \mu\text{m}$. The compounds were dissolved in chloroform at various concentrations ($(0-2) \times 10^{-2} \text{ mol L}^{-1}$). The centrosymmetry of the solution was broken by dipolar orientation of the chromophores with a high voltage pulse (around 5 kV) synchronized with the laser pulse. The second harmonic generation (SHG) signal was selected through a suitable interference filter, detected by a photomultiplier, and recorded on an ultrafast Tektronic TDS 620 B oscilloscope. With the NLO response being induced by dipolar orientation of the chromophores, the EFISH signal is therefore proportional to the dipole moment (μ) and to β_{vec} , the vector component of β along the dipole moment direction. However due to the C_2 symmetry of the molecules, β and μ are parallel, and therefore, β_{vec} and β are assumed to be equivalent. The dipole moments were measured independently by a classical method on the basis of the Guggenheim theory.³⁴ Further details on the experimental methodology and data analysis are reported elsewhere.³³

SHG measurements in the solid state were carried out by the Kurtz–Perry powder test,³⁵ using a nanosecond-pulsed Nd:YAG (10 Hz) laser. The fundamental radiation was used as the incident laser beam for SHG. The second harmonic signal was detected by a photomultiplier and read on an ultrafast Tektronic TDS 620B oscilloscope. The samples were uncalibrated microcrystalline powders obtained by grinding and put between two glass plates.

Results and Discussion

Synthesis and Characterization. The synthesis of Schiff base complexes based on 1,2-diamine is well documented (e.g. in catalytic asymmetric synthesis),³⁶ and therefore the mononuclear species have been obtained without any difficulties. The solutions of the copper complexes undergo a fast evolution from black to brown and from green to yellow-brown once the additions of Gd^{III} salts have been performed. This observation suggests the formation of the $\text{Cu}^{\text{II}}\text{Gd}^{\text{III}}$ binuclear species **1** and **2**, respectively. $\text{CuGdL}^2(\text{NO}_3)_3$ (**2**)

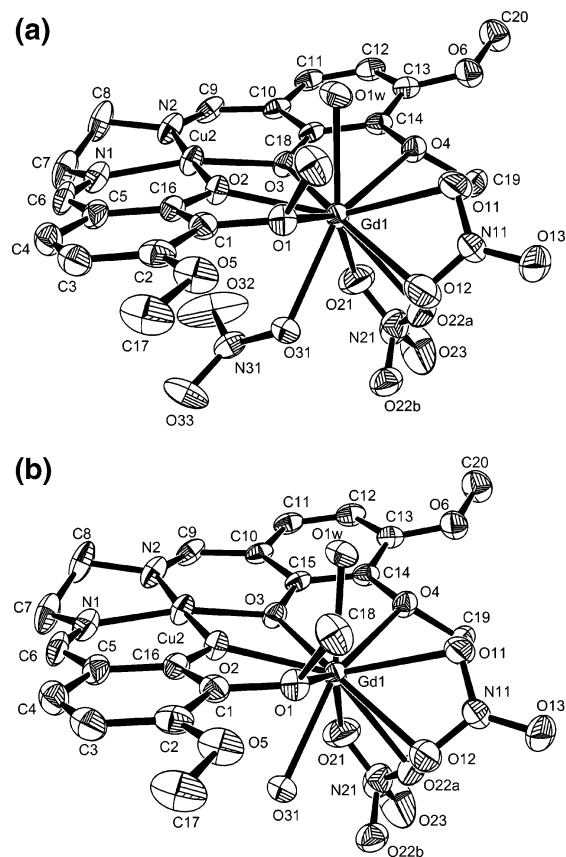


Figure 1. The two $\text{CuGdL}^1(\text{NO}_3)_3(\text{H}_2\text{O})$ (**1a**) and $\text{CuGdL}^1(\text{NO}_3)_2(\text{OH})(\text{H}_2\text{O})$ (**1b**) entities related through an inversion center in the unit cell of $\text{CuGdL}^1(\text{NO}_3)_{2.5}(\text{OH})_{0.5}(\text{H}_2\text{O}) \cdot 0.5\text{H}_2\text{O}$. The ellipsoids are drawn at the 50% probability level.

is readily obtained and characterized by elemental analysis and X-ray structure determination. After the drying of the powder under vacuum, elemental analysis and thermal analysis clearly show that no solvent is present in the compound. By contrast, the presence of acetone is evidenced in the crystal structure. Similarly, a complex of basic formula $\text{CuGdL}^1(\text{NO}_3)_3$ is normally expected from the reaction of $\text{CuL}^1 \cdot \text{H}_2\text{O}$ and $\text{Gd}(\text{NO}_3)_3 \cdot 6\text{H}_2\text{O}$. Instead, the crystal structure determination reveals a compound of formula $\text{CuGdL}^1(\text{NO}_3)_{2.5}(\text{OH})_{0.5}(\text{H}_2\text{O})$ (**1**), which results from the presence of two different complexes, $\text{CuGdL}^1(\text{NO}_3)_2(\text{OH})(\text{H}_2\text{O})$ and $\text{CuGdL}^1(\text{NO}_3)_3(\text{H}_2\text{O})$, in good agreement with the elemental analysis. This modification of the coordination sphere, which is not supposed to affect too strongly the NLO response and the magnetic properties, will be discussed in the next section.

Structural Studies. The molecular structure of $\text{CuGdL}^1(\text{NO}_3)_{2.5}(\text{OH})_{0.5} \cdot 1.5\text{H}_2\text{O}$ (**1**) and atom-labeling are shown in Figure 1. Crystallographically, the unit cell is built up from two equivalent complexes, which are related to each other through an inversion center. At first, the complexes appear connected through a possible $\text{Gd}^{\text{III}}-(\text{O}-\text{N}_2\text{O}_2-\text{O})^{2-}-\text{Gd}^{\text{III}}$ linkage, with a $\text{Gd}^{\text{III}} \cdots \text{Gd}^{\text{III}}$ distance equal to $8.029(2) \text{ \AA}$. This would imply the formation of the new $(\text{N}_2\text{O}_2)^{2-}$ anion (Chart 2a), an entity which has never been reported either experimentally or theoretically. A more careful examination of the X-ray data reveals that the weight of the two nitrogen

- (30) (a) Garge, P.; Chikate, R.; Padhye, S.; Savariault, J. M.; de Loth, P.; Tuchagues, J. P. *Inorg. Chem.* **1990**, *29*, 3315. (b) Aussoleil, J.; Cassoux, P.; de Loth, P.; Tuchagues, J. P. *Inorg. Chem.* **1989**, *28*, 3051.
- (31) James, F.; Roos, M. MINIUT Program, a System for Function Minimization and Analysis of the Parameters Errors and Correlations. *Comput. Phys. Commun.* **1975**, *10*, 345.
- (32) (a) Oudar, J. L. *J. Chem. Phys.* **1977**, *67*, 446. (b) Levine, B. F.; Betha, C. G. *J. Chem. Phys.* **1975**, *63*, 2666; **1976**, *65*, 1989.
- (33) Maltey, I.; Delaire, J. A.; Nakatani, K.; Wang, P.; Shi, X.; Wu, S. *Adv. Mater. Opt. Electron.* **1996**, *6*, 233.
- (34) Guggenheim, E. A. *Trans. Faraday Soc.* **1949**, *45*, 714.
- (35) (a) Kurtz, S. K.; Perry, T. T. *J. Appl. Phys.* **1968**, *39*, 3798. (b) Dougherty, J. P.; Kurtz, S. K. *J. Appl. Crystallogr.* **1976**, *9*, 145.
- (36) For examples of Jacobsen catalysts, see: (a) Palucki, M.; Pospisil, P. J.; Zhang, W.; Jacobsen, E. N. *J. Am. Chem. Soc.* **1994**, *116*, 9333. (b) Larrow, J. F.; Jacobsen, E. N. *J. Am. Chem. Soc.* **1994**, *116*, 12129.

Chart 2

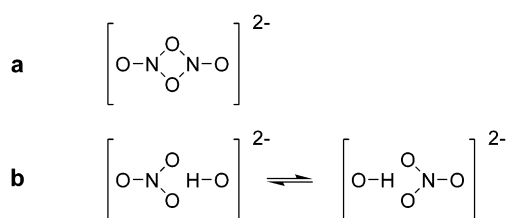


Table 2. Selected Bond Lengths (Å) and Angles (deg) for $\text{CuGdL}^1(\text{NO}_3)_2.5(\text{OH})_{0.5}(\text{H}_2\text{O}) \cdot 0.5\text{H}_2\text{O}$ (**1**) and $\text{CuGdL}^2(\text{NO}_3)_3 \cdot \text{C}_3\text{H}_6\text{O}$ (**2**), Where Esd's in Parentheses Refer to the Last Significant Digit

| Compound 1 | | | |
|------------------|------------|------------------|------------|
| Gd(1)–O(1) | 2.706(3) | Gd(1)–O(31) | 2.415(3) |
| Gd(1)–O(2) | 2.352(3) | Gd(1)–O(1w) | 2.374(3) |
| Gd(1)–O(3) | 2.339(3) | Gd(1)–Cu(2) | 3.378(2) |
| Gd(1)–O(4) | 2.660(3) | Cu(2)–O(2) | 1.896(3) |
| Gd(1)–O(11) | 2.490(4) | Cu(2)–O(3) | 1.907(3) |
| Gd(1)–O(12) | 2.512(5) | Cu(2)–N(1) | 1.917(4) |
| Gd(1)–O(21) | 2.473(5) | Cu(2)–N(2) | 1.911(4) |
| Gd(1)–O(22A) | 2.596(6) | | |
| Cu(2)–O(2)–Gd(1) | 104.85(13) | Cu(2)–O(3)–Gd(1) | 104.96(13) |
| Compound 2 | | | |
| Gd(1)–O(1) | 2.402(9) | Gd(1)–O(31) | 2.487(13) |
| Gd(1)–O(2) | 2.379(11) | Gd(1)–O(32) | 2.507(15) |
| Gd(1)–O(5) | 2.618(9) | Gd(1)–Cu(2) | 3.445(2) |
| Gd(1)–O(6) | 2.671(9) | | |
| Gd(1)–O(11) | 2.439(11) | Cu(2)–O(1) | 1.920(9) |
| Gd(1)–O(12) | 2.474(13) | Cu(2)–O(2) | 1.898(10) |
| Gd(1)–O(21) | 2.479(11) | Cu(2)–N(1) | 1.863(12) |
| Gd(1)–O(22) | 2.328(16) | Cu(2)–N(2) | 1.917(12) |
| Cu(2)–O(1)–Gd(1) | 105.2(4) | Cu(2)–O(2)–Gd(1) | 106.8(5) |

atoms is equal to 0.5 in the hypothetical $(\text{N}_2\text{O}_2)^{2-}$ anion, a structural feature which has rather to be ascribed to a disordered pair of NO_3^- and OH^- anions, in hydrogen bond interaction (Chart 2b).

The actual crystal indeed arises from a cocrystallization of $\text{CuGdL}^1(\text{NO}_3)_2(\text{OH})(\text{H}_2\text{O})$ and $\text{CuGdL}^1(\text{NO}_3)_3(\text{H}_2\text{O})$. The gadolinium ion is 10-coordinated (4 oxygens from L^1 , 4 oxygens from two bidentate NO_3^- , 1 oxygen from H_2O , and 1 oxygen from either OH^- or monodentate NO_3^-). The first coordination sphere is found to be the same for both entities, by virtue of the crystal symmetries. Selected bond lengths and angles are gathered in Table 2. The averaged Gd–O distance is equal to 2.492(4) Å, the longest bonds involving the OMe sidearms. The copper ion has a square planar coordination involving the N(1), N(2), O(2), and O(3) atoms and is located at 0.0075(2) Å out of their mean plane.

The molecular structure of $\text{CuGdL}^2(\text{NO}_3)_3 \cdot \text{C}_3\text{H}_6\text{O}$ (**2**) is shown in Figure 2, with the atom-labeling scheme. Two molecules of acetone are present in the asymmetric unit cell with an occupancy level of half. One of them is slightly interacting with the copper(II) ion, with a Cu(2)–O(1S) distance equal to 2.44(2) Å. Cu(II) is located at 0.153(6) Å above the O(1), O(2), N(1), N(2) mean plane, a value that is therefore larger than the 0.075 Å observed previously in the case of compound **1**. In the present $\text{CuGdL}^2(\text{NO}_3)_3$ complex, the gadolinium ion is 10-coordinated with an average Gd–O distance equal to 2.478(12) Å, the longest bonds involving the OMe sidearms. The three nitrate ions are bonded through two oxygen atoms.

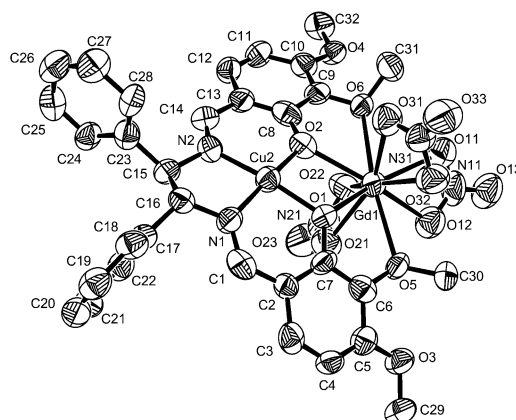


Figure 2. ORTEP view for the $\text{CuGdL}^2(\text{NO}_3)_3$ complex.

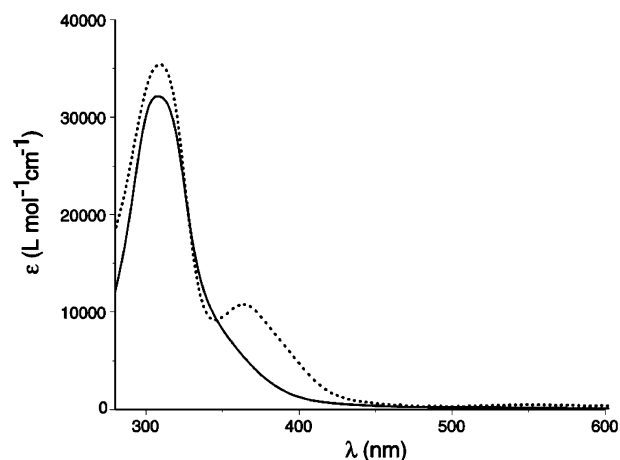


Figure 3. Optical spectra in CH_2Cl_2 of $\text{CuGdL}^2(\text{NO}_3)_3 \cdot \text{C}_3\text{H}_6\text{O}$, compared to that of $\text{CuL}^2 \cdot 0.5\text{H}_2\text{O}$ (dotted line).

Table 3. Experimental Spectroscopic Data (λ_{max} in nm, ϵ in $\text{L}^{-1} \text{mol}^{-1} \text{cm}^{-1}$) for the Binuclear and Related Mononuclear Species

| λ_{max} | ϵ | λ_{max} | ϵ |
|---|------------|--|------------|
| $\text{CuL}^1 \cdot \text{H}_2\text{O}$ | 306 | $\text{CuGdL}^1(\text{NO}_3)_2.5(\text{OH})_{0.5}(\text{H}_2\text{O})$ | 310 |
| | 35 300 | | 32 000 |
| | 362 | | 11 400 |
| $\text{CuL}^2 \cdot \text{H}_2\text{O}$ | 310 | $\text{CuGdL}^2(\text{NO}_3)_3$ | 310 |
| | 34 500 | | 34 515 |
| | 365 | | 11 450 |

Spectroscopic Properties. The experimental spectroscopic data for the $\text{Cu}^{\text{II}}\text{Gd}^{\text{III}}$ derivatives recorded in CH_2Cl_2 are gathered in Table 3 and compared to those of the parent mononuclear species. It clearly appears that both L^1 -based and L^2 -based complexes exhibit the same spectra, which indicates that the properties are dominated by the metal–salen electronic core. This feature completely agrees with an investigation previously reported.¹⁸ The modifications observed upon introduction of gadolinium are illustrated in Figure 3 in the case of the L^2 -containing chromophores. The copper(II) complex exhibits an intense transition localized around 310 nm, while a low lying but less intense band is present around 360 nm. This latter transition is absent in the binuclear $\text{Cu}^{\text{II}}\text{Gd}^{\text{III}}$ species.

A ZINDO investigation has been conducted to analyze the origin of these differences. Before discussing the results, it is important to remind here that the ZINDO-spectra analysis of open-shell molecules is not always fully reliable. Moreover, for high-spin ($S > 1$) molecules, like $\text{Cu}^{\text{II}}\text{Gd}^{\text{III}}$

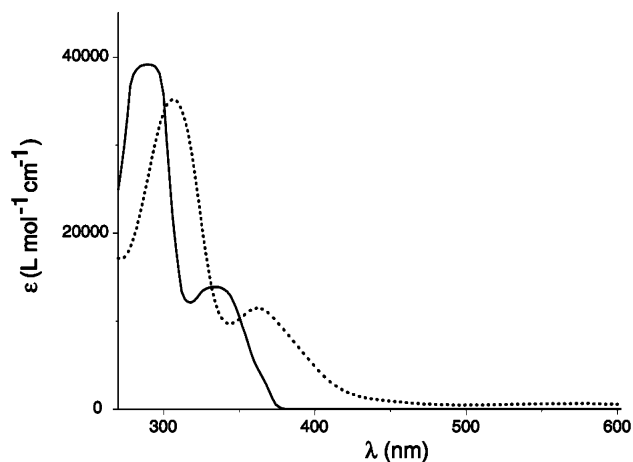


Figure 4. Calculated (ZINDO) spectrum for CuL^2 complex, compared to the experimental data (dotted line).

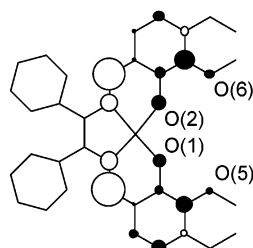


Figure 5. Difference in electronic populations between the ground state and the excited state for the calculated low-lying transition in the CuL^2 complex. The black (white) contribution indicates a decrease (increase) in electron density in the charge-transfer process.

complexes, the calculated spectra are not available using the present ZINDO release. Therefore, the calculation has been carried out on the ($S = 1/2$) mononuclear species, only. Both L^1 - and L^2 -based complexes exhibit similar calculated spectra; therefore, the data will be described here for CuL^2 , only. The calculated gas-phase spectrum is presented in Figure 4 and compared to the experimental one. Despite an energy difference of about 25 nm, the agreement between calculation and experimental data is satisfactory.

A more careful analysis of the calculated spectrum of CuL^2 reveals that the low-lying band actually results from two nearly degenerated transitions related to each other by the pseudosymmetry (2-fold axis) of the chromophore. More precisely, the charge-transfer associated with this transition is shown in Figure 5. It reveals that four oxygen atoms (labeled O(1), O(2), O(5), and O(6) in the crystal structure of $\text{CuGdL}^2(\text{NO}_3)_3 \cdot \text{C}_3\text{H}_6\text{O}$) (Figure 2) act as electron donor components in the transition. In the case of $\text{Cu}^{\text{II}}\text{Gd}^{\text{III}}$ species, these four atoms being linked to the gadolinium(III) center, one may suggest that most of the electron density available stays tightly located on the oxygen atoms. Consequently, the related transition might either be absent or shifted to much higher energy.

NLO Properties. The NLO efficiency of a molecular material is ultimately related to the underlying molecular hyperpolarizability (β). Therefore, before discussion of the bulk NLO response of the solid, it would be of great interest to evaluate precisely the β value of the present $\text{Cu}^{\text{II}}\text{Gd}^{\text{III}}$ derivatives. However, the direct β determination by the

Table 4. Experimental EFISH Data (μ in D, β in $\text{cm}^5 \text{esu}^{-1}$) for $\text{CuL}^1 \cdot \text{H}_2\text{O}$ and NiL^1

| | μ | β |
|---|-------|-------------------------|
| $\text{CuL}^1 \cdot \text{H}_2\text{O}$ | 6.0 | -6.5×10^{-30} |
| NiL^1 | 6.0 | -10.5×10^{-30} |

EFISH technique requires neutral species. In the present $\text{Cu}^{\text{II}}\text{Gd}^{\text{III}}$ complexes, the nitrate ions are partially labile in solution. Indeed, various experimental evidence (ionic conductivity,³⁷ NMR,³⁷ and mass spectra¹⁶) has previously pointed out that partial anion release is a general trend in bis(3-methoxysalicylaldiminato) 3d–4f metal complexes. In some cases, the cationic nature of these complexes has been observed in solid state as well.³⁸ Therefore, the nature and molecular structure of the species present in solution cannot be determined precisely, and direct β measurements are not available for the $\text{Cu}^{\text{II}}\text{Gd}^{\text{III}}$ derivatives.

Nevertheless, EFISH measurements have been performed on the neutral mononuclear $\text{CuL}^1 \cdot \text{H}_2\text{O}$ to evaluate the order of the β magnitude. The data are summarized in Table 4. The copper derivative exhibits a β value equal to $-6.5 \times 10^{-30} \text{ cm}^{-5} \text{esu}^{-1}$, which is surprisingly weaker than the $-9.6 \times 10^{-30} \text{ cm}^{-5} \text{esu}^{-1}$ value reported by Di Bella on a closely related bis(methoxysalicylaldiminato)nickel(II) derivative.^{17b} However, we have found that on passing from copper(II) to nickel(II) derivative (-10.5×10^{-30}), the agreement is more satisfactory, which seems to confirm the reduced NLO response for copper(II) complexes.

Within the framework of the SOS perturbation theory, β is usually related to a set of electronic transitions between the ground (g) and excited (e) states according to the 2-level expression³⁹

$$\beta = \sum_e \left(\frac{3e^2 \hbar^2 f_{ge} (\Delta\mu)_{ge}}{2mE_{ge}^3} \frac{E_{ge}^4}{(E_{ge}^2 - (2\hbar\omega)^2)(E_{ge}^2 - (\hbar\omega)^2)} \right) \quad (1)$$

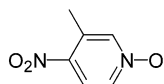
which relates the β value to the energy $\hbar\omega$ of the incident laser beam. In eq 1, E_{ge} is the energy, f_{ge} is the oscillator strength, and $\Delta\mu_{ge}$ is the change in dipole moment occurring in the $g \rightarrow e$ charge transfer transition. Although the above summation runs over all excited states of the chromophores, the intense and usually low-lying transitions are the only ones which possess a set of E , f , and $\Delta\mu$ parameters suitable for a sizable contribution to β . In the case of the mononuclear species, the high-intensity transition located around 310 nm is dominant in the NLO response (60% of the effect according to eq 1). The fact that this transition is present in both Cu^{II} and $\text{Cu}^{\text{II}}\text{Gd}^{\text{III}}$ spectra may tentatively be used to assume that both complexes possess β values lying roughly in the same order of magnitude. Nevertheless, any attempt to quantify β more precisely for the binuclear species would probably be somewhat unreliable, on the basis of these spectroscopic data only.

(37) Costes, J. P.; Laussac, J. P.; Nicodeme, F. *J. Chem. Soc., Dalton Trans.* **2002**, 2731.

(38) Costes, J. P.; Dahan, F.; Dupuis, A. *Inorg. Chem.* **2000**, *39*, 165.

(39) (a) Oudar, J. L.; Chemla, J. *J. Chem. Phys.* **1977**, *66*, 2664. (b) Oudar, J. L. *J. Chem. Phys.* **1977**, *67*, 446.

Chart 3



NLO Properties in the Solid State. In the case of $\text{Cu}^{\text{II}}\text{Gd}^{\text{III}}\text{L}^2(\text{NO}_3)_3$, the crystal being noncentrosymmetric ($P2_12_12_1$ orthorhombic space group), the efficiency in second harmonic generation has been measured and found to be equal to 0.3 times that of urea. It may be interesting to compare this value to that of 3-methyl-4-nitropyridine 1-oxide (POM, Chart 3), a molecular material commercially available, which crystallizes in the same $P2_12_12_1$ space group. POM has entered the market place in relation to its good transparency, its ability to be grown as very large single crystals,⁴⁰ and moreover a large efficiency equal to 13 times that of urea in second harmonic generation,⁴¹ a value 43 times larger than that of $\text{Cu}^{\text{II}}\text{Gd}^{\text{III}}\text{L}^2(\text{NO}_3)_3$. To find a rationale for this comparison, it must be remind that the SHG signal derives from the crystalline first-order nonlinearity $\chi^{(2)}$ (component d_{ijk} in the crystalline framework).⁴² Assuming a one-dimensional character, β has only one large tensor component (namely β_{xxx}) along the x symmetry axis of the molecule (Gd–Cu direction). In $P2_12_12_1$ (point group 222), the only nonvanishing component of $\chi^{(2)}$ is then

$$d_{XYZ} \propto (4/V)(\sin \phi)(\cos \phi)(\cos \theta)(\sin^2 \theta)\beta_{xxx} \quad (2)$$

where V is the volume cell and ϕ and θ are angular parameters defined from the Euler spherical angles.⁴² In POM, $V = 670 \times 10^{-24} \text{ cm}^3$, $\phi = 30.3^\circ$, $\theta = 58.6^\circ$, and $\beta_{xxx} = 8.5 \times 10^{-30} \text{ cm}^5 \text{ esu}^{-1}$. These parameters lead to $d_{XYZ} \propto 8.4 \times 10^{-9} \text{ esu}$. The assumption that the SHG efficiency is proportional to the nonvanishing $\chi^{(2)}$ tensor component leads to $d_{XYZ} \propto 2.0 \times 10^{-10} \text{ esu}$ ($= 8.4 \times 10^{-9}/43$) in $\text{Cu}^{\text{II}}\text{Gd}^{\text{III}}\text{L}^2(\text{NO}_3)_3 \cdot \text{C}_3\text{H}_6\text{O}$. Equation 2 in which $V = 4527 \times 10^{-24} \text{ cm}^3$, $\phi = 73^\circ$, and $\theta = 35.3^\circ$ leads to a β value around $3.0 \times 10^{-30} \text{ cm}^5 \text{ esu}^{-1}$, for the binuclear compound. This estimation of β is somewhat qualitative, as many additional parameters (e.g. level of crystallinity, Lorentz local field factors, phase matching ability) should be taken into account to reach the highest accuracy level in this comparison. Nevertheless, it seems to confirm that the mononuclear and binuclear species could have the same β magnitude.

Magnetic Properties. The magnetic behaviors have been investigated for both $\text{Cu}^{\text{II}}\text{Gd}^{\text{III}}$ complexes and found to be essentially similar. The temperature dependences of the magnetic properties are illustrated in Figure 6 for $\text{CuGdL}^1(\text{NO}_3)_{2.5}(\text{OH})_{0.5}(\text{H}_2\text{O}) \cdot 0.5\text{H}_2\text{O}$ in the form of the χT product vs T , χ being the molar magnetic susceptibility and T the temperature. At room temperature, χT is equal to $8.2 \text{ cm}^3 \text{ K mol}^{-1}$, a value which roughly corresponds to two isolated $S = 1/2$ ($\chi T = 0.375$) and $S = 7/2$ ($\chi T = 7.875$) ion, with a g value assumed to be equal to 2. As the temperature is lowered, the χT product remains constant until 100 K and

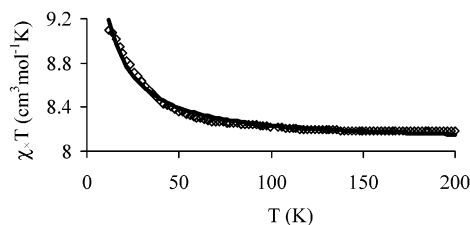


Figure 6. Experimental (diamond) and calculated (straight line) temperature dependence of χT for $\text{CuGdL}^1(\text{NO}_3)_{2.5}(\text{OH})_{0.5}(\text{H}_2\text{O}) \cdot 0.5\text{H}_2\text{O}$.

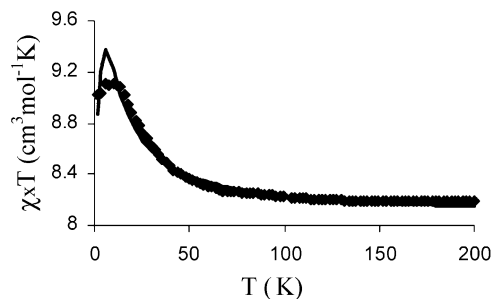


Figure 7. Experimental (diamond) and calculated (straight line) temperature dependence of χT for $\text{CuGdL}^1(\text{NO}_3)_{2.5}(\text{OH})_{0.5}(\text{H}_2\text{O}) \cdot 0.5\text{H}_2\text{O}$, assuming weak intermolecular interactions between binuclear species.

then slightly increases. This behavior reveals a ferromagnetic coupling between $S = 1/2$ and $S = 7/2$, with a $S = 4$ ground state.

A quantitative analysis has been performed on the basis of an expression derived from the exchange Hamiltonian $\hat{H} = -J S_{\text{Cu}} \cdot S_{\text{Gd}}$. This model treats the magnetic properties within the assumption of the isotropic interaction (Figure 7), which is by far the dominant magnetic phenomenon,⁴³ and has been previously used to account for various $\text{Cu}^{\text{II}}\text{Gd}^{\text{III}}$ interactions.^{16,37,38,44} The anisotropy of the copper(II) ion is expressed by the value of the g_{Cu} factor. Taking into consideration the g values associated with the low-lying levels $E(4) = 0$ and $E(3) = 4J$, $g_4 = (7g_{\text{Gd}} + g_{\text{Cu}})/8$, and $g_3 = (9g_{\text{Gd}} - g_{\text{Cu}})/8$,⁴⁵ we obtain the following theoretical expression:³⁸

$$\chi T = \frac{4N\mu_B^2}{k} \left[\frac{15g_4^2 + 7g_3^2 e^{-4J/kT}}{9 + 7e^{-4J/kT}} \right]$$

Here μ_B is the Bohr magneton. A least-squares fitting of the experimental data between 10 and 200 K (Figure 6) leads to $J = 3.0 \text{ cm}^{-1}$, $g_{\text{Cu}} = 2.10$, and $g_{\text{Gd}} = 1.98$ (agreement factor $R = 9 \times 10^{-4}$). Below 10 K, the χT product undergoes a slight decrease. Such a behavior may be due to interactions between heterobinuclear entities through the hydrogen-bonding linkage ($\text{Gd}^{\text{III}}-\text{NO}_3 \cdots \text{HO}-\text{Gd}^{\text{III}}$) and to a partial saturation of the large magnetic moment in the magnetic field, as observed before.^{38,44a} The possibility for a weak intermolecular interaction has been treated in the molecular field approximation, in which $T - \Theta$ is used instead of T

(43) Kahn, O. *Molecular Magnetism*; Wiley: New York, 1993; p 103.

(44) For other uses of $-J S_{\text{Cu}} \cdot S_{\text{Gd}}$, see, for example: (a) Costes, J. P.; Dahan, F.; Dupuis, A.; Laurent, J. P. *Inorg. Chem.* **1996**, *35*, 2400. (b) Ramade, I.; Kahn, O.; Jeannin, Y.; Robert, F. *Inorg. Chem.* **1997**, *36*, 930.

(45) Bencini, A.; Gatteschi, D. *EPR of Exchange Coupled Systems*; Springer-Verlag: Berlin, 1990.

(40) Hierle, R.; Badan, J. *Zyssh, J. J. Cryst. Growth* **1984**, *69*, 545.

(41) Zyssh, J.; Chemla, D. S. *J. Chem. Phys.* **1981**, *74*, 4800.

(42) Zyssh, J.; Oudar, J. L. *Phys. Rev. A* **1982**, *26*, 2028.

(Θ being the Weiss constant).⁴⁶ The fitting process yielded the following: $J = 3.3 \text{ cm}^{-1}$; $\Theta = -0.2 \text{ K}$; $g_{\text{Cu}} = 2.10$; $g_{\text{Gd}} = 1.99$ (agreement factor $R = 3 \times 10^{-3}$). Owing to the agreement factor, the improvement of the least-squares fitting is not significant with this later model, but it presents an advantage to fit the data on the overall temperature range. Nevertheless, it is important to point out that, in the case of a magnetic model implying an anisotropic g factor, the accuracy of the estimation of weak intermolecular interactions (Weiss constant) is somewhat approximative.

Similarly, the magnetic properties of $\text{Cu}^{\text{II}}\text{Gd}^{\text{III}}\text{L}^2(\text{NO}_3)_3 \cdot \text{C}_3\text{H}_6\text{O}$ reveal a χT product nearly constant between 300 and 50 K, which indicates a reduced coupling constant. As the temperature is further reduced, χT slightly increases up to $9.2 \text{ cm}^3 \text{ mol}^{-1} \text{ K}$ and then saturates below 10 K. The least-squares fitting of the experimental data from 10 to 200 K leads to $J = 1.3 \text{ cm}^{-1}$, $g_{\text{Cu}} = 2.10$, and $g_{\text{Gd}} = 2.01$ (agreement factor $R = 1 \times 10^{-3}$).

Conclusion

Two new $\text{Cu}^{\text{II}}\text{Gd}^{\text{III}}$ -based Schiff base complexes have been presented. For the first time an efficiency in second harmonic generation and a ferromagnetic coupling have been simultaneously observed in the solid state on the crystal of formula $\text{CuGdL}^2(\text{NO}_3)_3 \cdot \text{C}_3\text{H}_6\text{O}$, the origin of both properties being located on the same molecular entity. With this respect, the compound is, strictly speaking, a multiproperty molecular material.

(46) Kahn, O. *Molecular Magnetism*; Wiley: New York, 1993; p 27.

Finding a possible interplay between these properties on a single molecular unit raises interesting theoretical issues. The traditional approach in nonlinear optics is regarded within the framework of a dielectric subjected to an electric field. In this approach, no magnetic effect will interfere with the NLO response. At a deeper theoretical level, the framework could be enlarged to encompass both electric and magnetic dipole transitions, leading to generalized mixed electric–magnetic contributions to the NLO tensor.⁴⁷ This is out of the scope of the present investigation. Nevertheless, previous materials (e.g. molecular conductors) have occasionally benefit from the proximity of additional magnetic properties in the solid state.⁴⁸ There is no reason to think that interplays could not be envisioned in such materials with hybrid magneto-optical properties. A next step for these investigations is the increase of the range of magnetic interactions in the solid state. This is one of the topics currently being developed in our group.

Acknowledgment. The authors thank Dr A. Mari for his aid with the magnetic measurements.

Supporting Information Available: X-ray materials (atomic coordinates, interatomic distances, and bond angles) in pdf format. This material is available free of charge via Internet at <http://pubs.acs.org>.

IC049801J

(47) Wagniere, G. H. *Linear and Nonlinear Optical Properties of Molecules*; VCH: New York, 1993.

(48) Goze, F.; Laukhin, V. N.; Brossard, L.; Audouard, A.; Ulmet, J. P.; Askenazy, S.; Naito, T.; Kabayashi, H.; Kobayashi, M.; Cassoux, P. *Europhys. Lett.* **1994**, *28*, 427.